

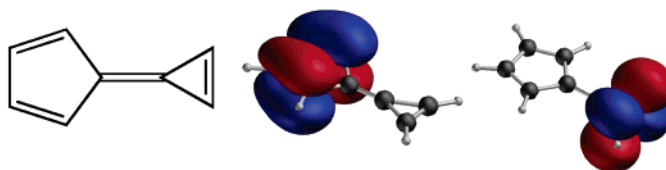
Quantum Chemical Characterization of Low-Energy States of Calicene in the Gas Phase and in Solution

Giovanni Ghigo,^{*,†} Abdul Rehaman Moughal Shahi,[‡] Laura Gagliardi,[‡] Lee M. Solstad,[§] and Christopher J. Cramer[§]

Dipartimento di Chimica Generale ed Organica Applicata, Università di Torino, C.so M. d'Azeglio 48, I-10125 Torino, Italy, Department of Physical Chemistry, Sciences II University of Geneva, 30 Quai Ernest Ansermet, CH-1211 Geneva 4, Switzerland, and Department of Chemistry and Supercomputer Institute, University of Minnesota, 207 Pleasant St. SE, Minneapolis, Minnesota 55455-0431

giovanni.ghigo@unito.it

Received November 24, 2006



The ground and excited electronic state properties of calicene (tripentafulvalene or 5-(cycloprop-2-en-1-ylidene)cyclopenta-1,3-diene) have been studied with a variety of density functional models (mPWPW91, PBE, TPSS, TPSh, B3LYP) and post-Hartree–Fock models based on single (MP2 and CCSD(T)) and multideterminantal (CASPT2) reference wave functions. All methods agree well on the properties of ground-state calicene, which is described as a conjugated double bond system with substantial zwitterionic character deriving from a charge-separated mesomer in which the three- and five-membered rings are both aromatic. Although the two rings are joined by a formal double bond, contributions from the aromatic mesomer reduce its bond order substantially. A rotational barrier of 40–41 kcal mol^{−1} is predicted in the gas phase and solvation effects reduce the barrier to 37 and 33 kcal mol^{−1} in benzene and water, respectively, because of increased zwitterionic character in the twisted transition-state structure. Multi-state CASPT2 (MS-CASPT2) is used to characterize the first few excited singlet and triplet states and indicates that the most important transition occurs at 4.93 eV (251 nm). A *cis*–*trans* photoisomerization about the inter-ring double bond is found to be inefficient.

Introduction

Calicene (tripentafulvalene or 5-(cycloprop-2-en-1-ylidene)cyclopenta-1,3-diene, **1**, Figure 1) is a completely conjugated unsaturated molecule.¹ To date, no synthesis of the parent compound has been successful,^{2,3} but several annelated and substituted derivatives have been prepared as targets or synthetic intermediates.^{3,4}

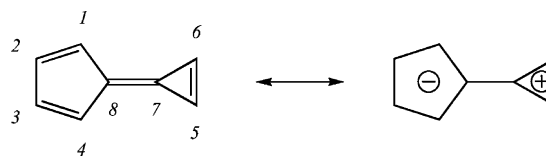


FIGURE 1. Calicene structure with atom numbering. The aromatic, zwitterionic mesomer is shown to the right.

The two unsaturated rings of calicene, joined by a double bond, can assume aromatic character in the limit of a dipolar mesomeric electronic structure. However, initial efforts varied widely in their estimate of this aromatic character.^{5,6} Subsequent to the original work of Roberts and Dewar, additional estimates

[†] University of Torino.

[‡] University of Geneva.

[§] University of Minnesota.

(1) Carey, F. A.; Sundberg, R. J. In *Advanced Organic Chemistry—Part A*, 4th ed.; Kluwer Academic/Plenum Publishers: New York, 2000; pp 539–540.

(2) von Mühlebach, M.; Neuenschwander, M. *Helv. Chim. Acta* **1994**, *77*, 1363–1376.

(3) Al-Dulayyimi, A.; Li, X.; Neuenschwander, M. *Helv. Chim. Acta* **2000**, *83*, 1633–1644 and references therein.

(4) See Halton, B. *Eur. J. Org. Chem.* **2005**, 3391–3414 and references therein.

(5) Roberts, J. D.; Streitwieser, A.; Regan, C. M. *J. Am. Chem. Soc.* **1952**, *74*, 4579–4582.

(6) Dewar, M. J. S.; Gleicher, G. J. *Tetrahedron* **1965**, *21*, 3423–3427.

derived from modeling at semiempirical^{7–11} and ab initio^{12–14} levels of theory were reported. Most of these calculations predict the geometry of calicene to be essentially that of a delocalized polyene, with calculated bond distances in good agreement with available X-ray data for 1,2,3,4-tetrachloro-5,6-di-*n*-propylcalicene¹⁵ and 1,2,3,4-tetrachloro-5,6-diphenylcalicene.¹⁶ However, the degree of bond alternation in calicene is very low compared to that found for other fulvenes and fulvalenes.^{8,13} The resonance energy associated with significant contributions from the zwitterionic structure has been computed to be quite high,^{10,11} suggesting that the three- and five-membered rings are highly aromatized as cyclopropenium and cyclopentadienide moieties, respectively.

The significance of the zwitterionic mesomer is also evident in the high electrical dipole moments determined experimentally for some substituted calicenes. Thus, a value of 6.3 D was found for hexaphenylcalicene,¹⁷ 7.56 D for 1,2,3,4-tetrachloro-5,6-di-*n*-propylcalicene,¹⁸ and 8.1 D for 1,2,3,4-tetrachloro-5,6-diphenylcalicene.¹⁹ Calculated dipole moments for parent calicene **1** range from 4.3 to 5.6 D,^{7,11,13,20,21} and a value of 5.63 D was estimated from an analysis of experimental data for analogous molecules.¹⁸

Because the zwitterionic mesomer of **1** has a formal single bond connecting the two rings, a measure of the importance of this resonance contributor should be reflected in the rotational barrier about this bond. The measured barrier for rotation of one ring relative to the other in 1-formyl-5,6-di-*n*-propylcalicene is 18–19 kcal mol^{–1},²² which may be compared to 65 kcal mol^{–1} for ethylene and 46 kcal mol^{–1} for stilbene.²³ The first calculations on the rotational barrier were performed in 1972²⁴ and predicted a value of 27 kcal mol^{–1}. A subsequent semiempirical prediction of more than 55 kcal mol^{–1} was recognized as unlikely to be accurate,²⁵ although a later calculation at the Hartree–Fock (HF) level predicted a barrier of 44 kcal mol^{–1}.¹¹ Substituent effects were estimated to have influences of 10–30% on the computed rotational barriers. High-level calculations are still lacking for this rotational barrier and the influence of

substituents and solvent effects thereupon; these are undertaken as part of this work.

The properties of calicene excited states have also been of some interest, although comprehensive studies are lacking. The lower singlet excited states have been studied only with semiempirical methods,^{7,8,21} (to include some study of the potential energy surface for the first excited singlet⁹), and in certain instances comparisons have been made to experimental data for substituted calicenes.^{21,26} Higher level density functional theory (DFT) and multireference second-order perturbation theory (CASPT2) calculations have also been reported for the lowest energy quintet state.²⁰ In this work, we characterize the excited states of calicene, including solvatochromic effects, using various density functional and wave function based models. We also examine *cis*–*trans* photoisomerization about the inter-ring double bond in the excited-state singlet S1.

Methods

Density Functionals. Geometries for the planar and twisted conformations of calicene were fully optimized with a variety of functionals using the 6-311G(2d,p) basis set.²⁷ We chose, in particular, the *m*PWPW,²⁸ PBE,²⁹ TPSS,³⁰ TPSSH,³¹ and B3LYP³² functionals. We thus include entirely local generalized gradient approximation (GGA) functionals (*m*PWPW and PBE), a hybrid functional incorporating HF exchange (B3LYP), a meta-GGA functional including a dependence on kinetic energy density (TPSS), and a hybrid meta-GGA functional (TPSSH).

Solvation effects were included via the conductor-like polarizable continuum model³³ (CPCM) employing the same basis set and united-atom radii optimized for this model (UAHF). Geometries were re-optimized in solution.

Electronic excitation energies were computed by time-dependent (TD) DFT. For TD-DFT calculations, diffuse functions²⁷ on the heavy atoms were added to the basis set.

Single-Reference Post-Hartree–Fock Models. Geometries for the planar and the 90°-rotated geometries of calicene (both belonging to the C_{2v} point group) were also fully optimized at the second-order perturbation theory (MP2) level³⁴ using the 6-311G(2d,p) basis set. Single point energies at these geometries were computed at the coupled-cluster level including all single and double excitations and a perturbative estimate for triple excitations (CCSD(T)).³⁵

(7) Nakajima, T.; Kohda, S.; Tajiri, A.; Karasawa, S. *Tetrahedron* **1967**, 23, 2189–2194.

(8) Nakajima, T. *Pure Appl. Chem.* **1971**, 28, 219–238.

(9) Takahashi, O.; Kikuchi, O. *Tetrahedron* **1990**, 46, 3803–3812.

(10) Aihara, J. *J. Chem. Soc., Perkin Trans.* **1966**, 2, 2185–2195.

(11) Hess, B. A., Jr.; Schaad, L. J. *J. Am. Chem. Soc.* **1971**, 93, 305–310.

(12) Hess, B. A., Jr.; Schaad, L. J.; Ewig, C. S.; Cársky, P. *J. Comput. Chem.* **1983**, 4, 53–57.

(13) Scott, A. P.; Agranat, I.; Biedermann, P. U.; Riggs, N. V.; Radom, L. *J. Org. Chem.* **1997**, 62, 2026–2038.

(14) Apeloig, Y.; Boese, R.; Halton, B.; Maulits, A. H. *J. Am. Chem. Soc.* **1998**, 120, 10147–10153.

(15) Shimanouchi, H.; Ashida, T.; Sasada, Y.; Kakudo, M.; Murata, I.; Kitahara, Y. *Tetrahedron Lett.* **1967**, 61–66.

(16) Kennard, O.; Watson, D. G.; Facocett, J. K.; Kerr, K. A.; Romers, C. *Tetrahedron Lett.* **1967**, 3885–3887.

(17) Bergmann, E. D.; Agranat, I. *J. Chem. Soc., Chem. Commun.* **1965**, 21, 512–513.

(18) Kitahara, Y.; Murata, I.; Ueno, M.; Sato, K. *J. Chem. Soc., Chem. Commun.* **1966**, 22, 180.

(19) Bergmann, E. D.; Agranat, I. *Tetrahedron* **1966**, 22, 1275–1278.

(20) Möllerstedt, H.; Piqueras, M. C.; Crespo, R.; Ottosson, H. *J. Am. Chem. Soc.* **2004**, 126, 13938–13939.

(21) Groenen, E. J. *Mol. Phys.* **1978**, 36, 1555–1564.

(22) Kende, A. S.; Izzo, P. T.; Fulmor, W. *Tetrahedron Lett.* **1966**, 31, 3967–3703.

(23) Lin, M. C.; Laidler, K. J. *Can. J. Chem.* **1968**, 46, 973–978.

(24) Dewar, M. J. S.; Kohn, M. C. *J. Am. Chem. Soc.* **1972**, 94, 2699–2704.

(25) Gleicher, G. J.; Arnold, J. C. *Tetrahedron* **1973**, 29, 513–517.

(26) Kende, A. S.; Izzo, P. T.; MacGregor, P. T. *J. Am. Chem. Soc.* **1966**, 88, 3359–3366.

(27) Hehre, W. J.; Radom, L.; Schleyer, P. v. R.; Pople, J. A. *Ab Initio Molecular Orbital Theory*; Wiley: New York, 1986.

(28) Perdew, J. P.; Wang, Y. *Phys. Rev. B* **1986**, 33, 88008802. Perdew, J. P. In *Electronic Structure of Solids '91*; Ziesche, P., Eschrig, H., Eds.; Akademie Verlag: Berlin, 1991; p 11. Adamo, C.; Barone, V. *J. Chem. Phys.* **1998**, 108, 664–675.

(29) Perdew, J. P.; Burke, K.; Enzerhof, M. *Phys. Rev. Lett.* **1996**, 77, 3865–3868.

(30) Tao, J.; Perdew, J. P.; Staroverov, V. N.; Scuseria, G. E. *Phys. Rev. Lett.* **2003**, 91, 146401.

(31) Staroverov, V. N.; Scuseria, G. E.; Tao, J.; Perdew, J. P. *J. Chem. Phys.* **2003**, 119, 12137.

(32) Becke, A. D. *Phys. Rev. A* **1988**, 38, 3098–3100. Lee, C.; Yang, W.; Parr, R. G. *Phys. Rev. B* **1988**, 37, 785–789. Becke, A. D. *J. Chem. Phys.* **1993**, 98, 5648–5652. Stephens, P. J.; Devlin, F. J.; Chabalowski, C. F.; Frisch, M. J. *J. Phys. Chem.* **1994**, 98, 11623–11627.

(33) Barone, V.; Cossi, M. *J. Phys. Chem. A* **1998**, 102, 1995; Cossi, M.; Rega, N.; Scalmani, G.; Barone, V. *J. Comput. Chem.* **2003**, 24, 669–681.

(34) Head-Gordon, V. M.; Head-Gordon, T. *Chem. Phys. Lett.* **1994**, 220, 122–128.

(35) Pople, J. A.; Head-Gordon, M.; Raghavachari, K. *J. Chem. Phys.* **1987**, 87, 5968–5975.

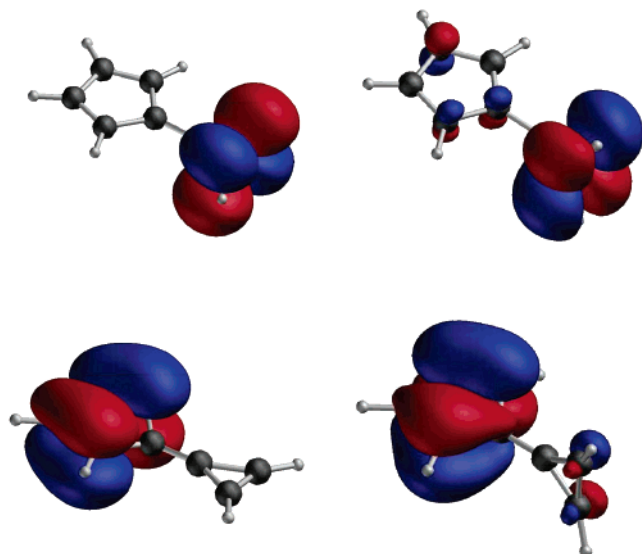


FIGURE 2. LUMOs (top) and HOMOs (bottom) for the equilibrium (left) and TS structure (right) of **1** at the B3LYP level.

Multiconfigurational Models. The complete active space (CAS) SCF method³⁶ was used to generate molecular orbitals and reference wave functions for subsequent multiconfigurational second-order perturbation calculations of the dynamic correlation energy (CASPT2).^{37–39} The active space was composed of the eight electrons and orbitals of the π system. The CASPT2 calculations used a new level-shift technique that shifts active orbital energies in order to simulate ionization energies for orbitals excited out of and electron affinities for orbitals excited into. This technique has recently been shown to reduce the systematic error in the CASPT2 approach for processes where the number of closed-shell electron pairs changes.⁴⁰

Geometries for the planar and twisted conformations (torsional angle ω from 0° to 90°, 15° steps) of ground state calicene were fully optimized at the CASPT2 level with numerical gradients. A general atomic natural orbital (ANO) contraction scheme of 3s2p1d on C and 2s1p on H was used for the basis set.⁴¹ For the planar and the twisted TS structures only, the same ANO-L basis set was used with a contraction scheme of 4s3p2d and 3s1p. This basis set is thus similar to the 6-311G(2d,p) basis set used for the other methods.

For the seven geometries along the rotational coordinate, the ground state and the first excited singlet and triplet A and B states were calculated at the multistate CASPT2 (MS-CASPT2) level.⁴² In order to minimize the effect of weakly interacting intruder states, a level shift of 0.25 au was employed.^{43,44} The basis set for these calculations was contracted 4s3p1d on C and 2s1p on H.

(36) Roos, B. O. In *Advances in Chemical Physics, Ab Initio Methods in Quantum Chemistry*; Lawley, K. P., Ed.; Wiley: Chichester, England, 1987; Vol. 2, pp 399–445.

(37) Andersson, K.; Malmqvist, P.-Å.; Roos, B. O.; Sadlej, A. J.; Wolinski, K. *J. Phys. Chem.* **1990**, *94*, 5483–5488.

(38) Andersson, K.; Malmqvist, P.-Å.; Roos, B. O. *J. Chem. Phys.* **1992**, *96*, 1218–1226.

(39) Roos, B. O.; Andersson, K.; Fülcher, M. P.; Malmqvist, P.-Å.; Serrano-Andrés, L.; Pierloot, K.; Merchán, M. In *Advances in Chemical Physics, New Methods in Computational Quantum Mechanics*; Prigogine, I., Rice, S. A., Ed.; Wiley: New York, 1996; Vol. 93, pp 219–331.

(40) Ghigo, G.; Roos, B. O.; Malmqvist, P.-Å. *Chem. Phys. Lett.* **2004**, *396*, 142–149.

(41) Pierloot, K.; Dumez, B.; Widmark, P.-O.; Roos, B. O. *Theor. Chim. Acta* **1995**, *90*, 87–114.

(42) Finley, J.; Malmqvist, P.-Å.; Roos, B. O.; Serrano-Andrés, L. *Chem. Phys. Lett.* **1998**, *288*, 299–306.

(43) Roos, B. O.; Andersson, K. *Chem. Phys. Lett.* **1995**, *245*, 215–223.

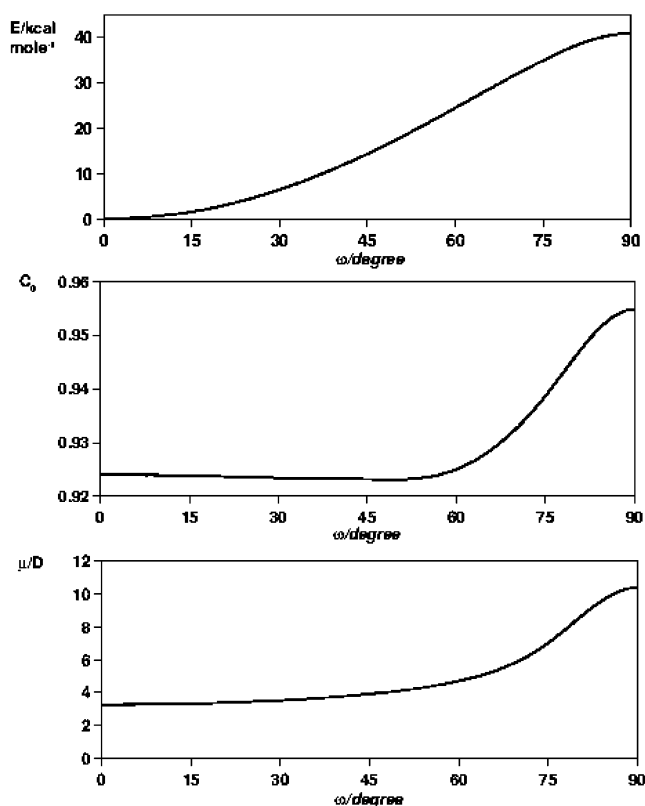


FIGURE 3. (Top) Rotational coordinate (kcal mol^{−1}) for **1** at the CASPT2 level. (Middle) Coefficient (C_0) of dominant aufbau configuration in the CASSCF wave function. (Bottom) Dipole moment (D) of **1** at the CASPT2 level.

For the planar and twisted TS structures, CASSCF/MS-CASPT2 calculations were performed in which solvent effects on the various electronic states were included by a self-consistent reaction field (SCRF) procedure. The nonequilibrium polarizable continuum model (PCM)⁴⁵ was used for the reaction field. In this approach the slow component of the solvent response is frozen to its equilibrium response to the ground state. The fast (optical) part of the solvent response relaxes self-consistently in response to the state of interest. Both water and benzene were considered as solvents.

Software. All DFT, MP2, and CCSD(T) calculations were performed using the Gaussian 03 suite of electronic structure programs.⁴⁶ All multireference calculations were performed using MOLCAS-6.4.⁴⁷ Figures 4 and 5 were generated by the MOLDEN visualization program.⁴⁸

(44) Roos, B. O.; Andersson, K.; Fülcher, M. P.; Serrano-Andrés, L.; Pierloot, K.; Merchán, M.; Molina, V. *J. Mol. Struct.: THEOCHEM* **1996**, *388*, 257–276.

(45) Cossi, M.; Barone, V. *J. Phys. Chem. A* **2000**, *104*, 10614–10622.

(46) Frisch, M. J.; Trucks, G. W.; Schlegel, H. B.; Scuseria, G. E.; Robb, M. A.; Cheeseman, J. R.; Montgomery, Jr., J. A.; Vreven, T.; Kudin, K. N.; Burant, J. C.; Millam, J. M.; Iyengar, S. S.; Tomasi, J.; Barone, V.; Mennucci, B.; Cossi, M.; Scalmani, G.; Rega, N.; Petersson, G. A.; Nakatsuji, H.; Hada, M.; Ehara, M.; Toyota, K.; Fukuda, R.; Hasegawa, J.; Ishida, M.; Nakajima, T.; Honda, Y.; Kitao, O.; Nakai, H.; Klene, M.; Li, X.; Knox, J. E.; Hratchian, H. P.; Cross, J. B.; Bakken, V.; Adamo, C.; Jaramillo, J.; Gomperts, R.; Stratmann, R. E.; Yazyev, O.; Austin, A. J.; Cammi, R.; Pomelli, C.; Ochterski, J. W.; Ayala, P. Y.; Morokuma, K.; Voth, G. A.; Salvador, P.; Dannenberg, J. J.; Zakrzewski, V. G.; Dapprich, S.; Daniels, A. D.; Strain, M. C.; Farkas, O.; Malick, D. K.; Rabuck, A. D.; Raghavachari, K.; Foresman, J. B.; Ortiz, J. V.; Cui, Q.; Baboul, A. G.; Clifford, S.; Cioslowski, J.; Stefanov, B. B.; Liu, G.; Liashenko, A.; Piskorz, P.; Komaromi, I.; Martin, R. L.; Fox, D. J.; Keith, T.; Al-Laham, M. A.; Peng, C. Y.; Nanayakkara, A.; Challacombe, M.; Gill, P. M. W.; Johnson, B.; Chen, W.; Wong, M. W.; Gonzalez, C.; Pople, J. A. *Gaussian 03*; Gaussian, Inc.: Wallingford CT, 2004.

TABLE 1. Predicted Rotational Activation Energies for **1** at Different Theoretical Levels^a

property	level						
	mPWPW91	PBE	TPSS	TPSSh	B3LYP	CASPT2	MP2
Im(ν^\ddagger)	463	459	457	484	459	<i>b</i>	410
ΔE^\ddagger	39.5	39.4	39.9	40.5	41.3	40.6	41.2
ΔG^\ddagger	36.2	36.1	36.8	37.7	38.3	<i>b</i>	39.6

^a See Methods for description of basis sets. Im(ν^\ddagger) in cm⁻¹. ΔE^\ddagger and ΔG^\ddagger in kcal mol⁻¹. ^b Not computed.

TABLE 2. Properties of Planar **1** in Benzene and Aqueous Solution at the CPCM/PBE Level (See Figure 1 for Atom Numbering)^a

property	solvent	
	benzene	water
<i>r</i> 12	1.371	1.375
<i>r</i> 23	1.453	1.451
<i>r</i> 48	1.455	1.453
<i>r</i> 56	1.330	1.333
<i>r</i> 67	1.428	1.422
<i>r</i> 78	1.358	1.364
<i>ab</i> -5	0.083	0.077
<i>ab</i> -3	0.098	0.089
$\Delta q/e$	0.475	0.552
μ/D	5.16	6.43
ΔG_s	-0.4	-4.2

^a See Methods for description of basis sets. Bond distances (*r*) and bond alternation parameters for five-membered (*ab*-5) and three-membered (*ab*-3) rings are in Å. Charge transfer (Δq) refers to the total charge difference between the atoms in the 5-membered ring and those in the 3-membered ring as computed from Mulliken charges. ΔG_s is the solvation free energy in kcal mol⁻¹.

Results and Discussion

Gas-Phase Calculations of Electronic Ground State. We first present results for the electronic ground state of **1**, which is ¹A. The minimum energy geometry for **1** has all atoms in a plane; geometrical details and electrical properties as a function of theory are listed in Supporting Information, page S25. The DFT geometries are sensitive to incorporation of Hartree–Fock (HF) exchange in the functional, with pure DFT functionals exhibiting bond lengths that are a few thousandths of an angstrom longer than those from the hybrid functionals, and the difference increases with increasing amounts of HF exchange. The effect is fairly small in magnitude, however, and in general there is very good agreement between DFT, CASPT2, and MP2 for the various bond lengths (the standard deviation is less than 0.01 Å). Noting that substituents will have some influence on bond lengths in the two calicenes for which X-ray data are available, comparison of these data to the calculated bond distances is also reasonable, with standard deviations of less than 0.03 Å. All levels predict there to be substantial bond alternation, e.g., *r*12 ≈ 1.36 – 1.37 Å; *r*23, *r*48, and *r*67 ≈ 1.42–1.46 Å; *r*56 ≈ 1.42–1.43 Å, and also that the length of the bond connecting the two rings (*r*78 ≈ 1.35 Å) is fairly typical for a double bond, consistent with the non-zwitterionic mesomeric structure.

(47) Karlström, G.; Lindh, R.; Malmqvist, P.-Å.; Roos, B. O.; Ryde, U.; Veryazov, V.; Widmark, P.-O.; Cossi, M.; Schimmelpfennig, B.; Neogrady, P.; Seijo, L. *Comput. Mater. Sci.* **2003**, 28, 222–239. Veryazov, V.; Widmark, P.-O.; Serrano-Andrés, L.; Lindh, R.; Roos, B. O. *Int. J. Quantum Chem.* **2004**, 100, 626–635.

(48) Schaftenaar, G.; Noordik, J. H. *J. Comput.-Aided Mol. Des.* **2000**, 14, 123–134.

(49) Mulliken, R. S. *J. Chem. Phys.* **1955**, 23, 1833–1840.

(50) Cioslowski, J. *J. Am. Chem. Soc.* **1989**, 111, 8333–8336.

TABLE 3. Properties of Twisted TS Structure of **1** in Benzene and Aqueous Solution at the CPCM/PBE Level (See Figure 1 for Atom Numbering)^{a,b}

property	solvent	
	benzene	water
<i>r</i> 12	1.405	1.407
<i>r</i> 23	1.411	1.414
<i>r</i> 48	1.430	1.428
<i>r</i> 56	1.357	1.357
<i>r</i> 67	1.397	1.393
<i>r</i> 78	1.404	1.416
<i>ab</i> -5	0.018	0.017
<i>ab</i> -3	0.040	0.036
$\Delta q/e$	0.731	0.867
μ/D	9.28	11.68
ΔG_s	-2.5	-11.0

^a See Methods for description of basis sets. Bond distances (*r*) and bond alternation parameters for five-membered (*ab*-5) and three-membered (*ab*-3) rings are in Å. Charge transfer (Δq) refers to the total charge difference between the atoms in the five-membered ring and those in the five-membered ring as computed from Mulliken charges. ΔG_s is the solvation free energy in kcal mol⁻¹. ^b Distances for *C_s* structures are averaged over the two bonds that would otherwise be equivalent in *C_{2v}* symmetry.

TABLE 4. Electronic States of Planar **1** at the MS-CASPT2 Level^a

state	<i>E</i>	TDM	<i>f</i>	T	μ
1- ¹ A					3.30
2- ¹ A	3.83	0.078	0.001	1 <i>a</i> → 2 <i>a</i>	-2.68
3- ¹ A	4.93	1.645	0.327	3 <i>b</i> → 4 <i>b</i>	4.92
1- ¹ B	3.84	0.263	0.007	3 <i>b</i> → 2 <i>a</i>	-1.93
2- ¹ B	4.03	0.391	0.015	1 <i>a</i> → 4 <i>b</i>	1.30
1- ³ A	3.40	0	0	3 <i>b</i> → 4 <i>b</i>	2.01
2- ³ A	3.86	0	0	1 <i>a</i> → 2 <i>a</i>	-2.80
1- ³ B	2.85	0	0	1 <i>a</i> → 4 <i>b</i>	1.44
2- ³ B	3.34	0	0	3 <i>b</i> → 2 <i>a</i>	-1.15

^a Excitation energies in eV; CASSCF transition dipole moment TDM; oscillator strength *f*; electronic transition T in the dominant configuration in the CASSCF wavefunction (for labels see Figure 4); state-averaged CASSCF dipole moment μ in debye.

On the other hand, consistent with the importance of the zwitterionic mesomer, there is substantial charge transfer between the two rings, as measured by either Mulliken population analysis⁴⁹ (with which the charge separation is estimated as 0.4–0.5 e depending on theoretical level; atomic polar tensor analysis,⁵⁰ which tends to be less sensitive to basis set effects than does Mulliken analysis, gave slightly larger DFT charges); or computed dipole moments that are around 4.5 D depending on level of theory (Supporting Information). This value is within the range of previously estimated values.^{7,12,13,18,20,21}

Electrical properties and geometrical data for transition state (TS) structures associated with rotation about the bond joining the two rings are provided in Supporting Information, page S26. DFT predicts in every case that the TS structure has *C_s* and not *C_{2v}* symmetry. The lowering of the symmetry involves a very small pyramidalization of one carbon atom in the inter-ring bond. However, the energetics associated with this pyramidalization are very small, ranging from 0.003 kcal mol⁻¹ for

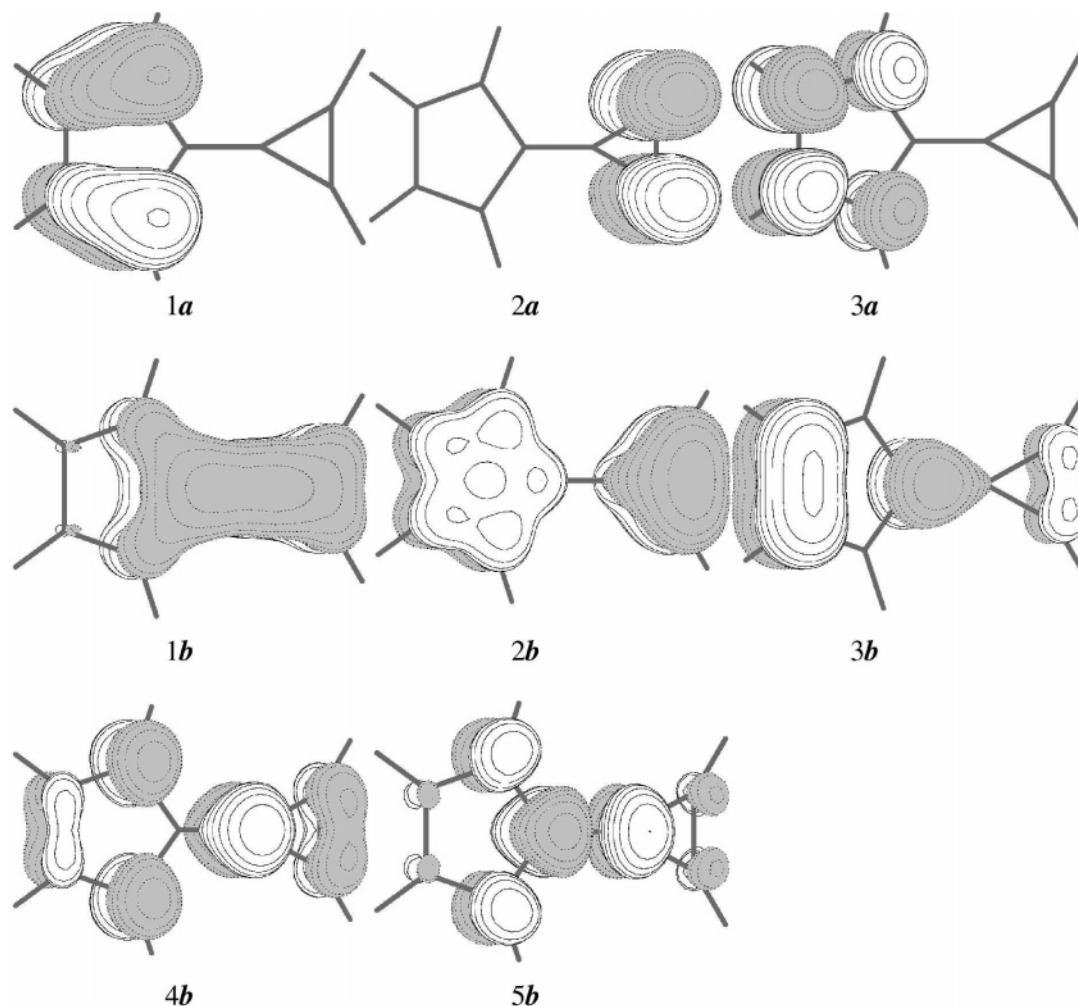


FIGURE 4. Molecular orbitals in the active space for planar calicene.

TABLE 5. Electronic States of Twisted TS Structure of 1 at the MS-CASPT2 Level^a

state	<i>E</i>	T	μ
1- ¹ A	1.96		11.29
2- ¹ A	3.16	3 <i>b</i> → 4 <i>b</i>	0.32
3- ¹ A	3.59	1 <i>a</i> → 2 <i>a</i>	-1.46
1- ¹ B	3.45	3 <i>b</i> → 2 <i>a</i>	-1.08
2- ¹ B	3.54	1 <i>a</i> → 4 <i>b</i>	0.72
1- ³ A	3.28	3 <i>b</i> → 4 <i>b</i>	0.99
2- ³ A	3.64	1 <i>a</i> → 2 <i>a</i>	-1.29
1- ³ B	3.38	3 <i>b</i> → 2 <i>a</i>	-1.05
2- ³ B	3.47	1 <i>a</i> → 4 <i>b</i>	0.72

^a Energies with respect to the planar ground state in eV; electronic transition T in the dominant configuration in the CASSCF wavefunction (for labels see Figure 5); state-averaged CASSCF dipole moment μ in debye.

TABLE 6. Properties of Planar 1 at the MS-CASPT2 Level in Gas, Benzene, and Water^a

state	<i>E</i> gas	μ gas	<i>E</i> benzene	μ benzene	<i>E</i> water	μ water
1- ¹ A		3.30		3.85		5.06
2- ¹ A	3.83	-2.68	4.09	-2.21	4.45	-1.21
3- ¹ A	4.93	4.92	4.83	5.92	4.73	7.67
1- ¹ B	3.84	-1.93	3.92	-2.28	4.04	-2.58
2- ¹ B	4.03	1.30	<i>b</i>	<i>b</i>	<i>b</i>	<i>b</i>
1- ³ A	3.40	2.01	3.51	2.26	3.69	1.89
2- ³ A	3.86	-2.80	3.93	-2.53	4.00	-2.94
1- ³ B	2.85	1.44	2.93	1.61	3.06	1.47
2- ³ B	3.34	-1.15	3.41	-0.96	3.54	-1.11

^a Excitation energies *E* in eV; state-averaged CASSCF dipole moment μ in debye. ^b Not converged.

B3LYP to 0.3 kcal mol⁻¹ for *m*PWPW91, suggesting that the TS structure may be regarded as effectively *C*_{2*v*}. The driving force for the symmetry reduction appears to be associated with a slight decrease in polarity. Thus, the electrical dipole moments in the *C*_s symmetric structures are from 0.05 to 0.78 D smaller than those for the *C*_{2*v*} symmetric structures.

The CC bond distances in the five-membered ring are all similar and span from 1.40 to 1.43 Å. As a comparison, the value obtained with the same methods for the aromatic cyclopentadienyl anion is 1.42 Å. In the three-membered ring some bond alternation is still present (*r*₅₆ ≈ 1.36 Å; *r*₆₇ ≈

1.42 Å), but the short CC bond distance is close to the value obtained for the aromatic cyclopropenyl cation (1.37 Å). Although intra-ring bond distances are consistent with the dominance of the aromatic mesomer in the TS structure, the *inter*-ring CC bond is clearly shorter than a single bond (1.40 Å). Of course, it is important to note that the single bond in question is between two formally sp² carbon atoms. Thus, appropriate reference systems might be biphenyl or *s*-*cis* butadiene (where in each case the conjugated systems on either side of the connecting single bond are forced to be twisted relative to one another by steric constraints). At the B3LYP/

TABLE 7. Properties of Twisted TS Structure **1** at the MS-CASPT2 Level in Gas, Benzene, and Water^a

state	<i>E</i> gas	μ gas	<i>E</i> benzene	μ benzene	<i>E</i> water	μ water
1- ¹ A		11.29		13.19		12.63
2- ¹ A	3.16	0.32	3.24	1.65	3.30	1.24
3- ¹ A	3.59	-1.46	3.70	-0.62	<i>b</i>	<i>b</i>
1- ¹ B	3.45	-1.08	3.54	-1.19	3.62	-1.35
2- ¹ B	3.54	0.72	3.60	0.61	<i>b</i>	<i>b</i>
1- ³ A	3.28	0.99	3.38	1.08	3.52	0.90
2- ³ A	3.64	-1.29	3.70	-1.19	3.81	-1.29
1- ³ B	3.38	-1.05	3.47	-1.16	3.61	-1.06
2- ³ B	3.47	0.72	3.54	0.61	3.64	0.70

^a Excitation energies *E* in eV; state-averaged CASSCF dipole moment μ in debye. ^b Not converged.

6-311G(2d,p) level, the central single bond lengths are computed to be 1.484 and 1.467 Å.

Inspection of the molecular orbitals for the planar and twisted structures provides key information on their electronic structures and helps to rationalize the short single bond in the twisted TS structure. As shown in Figure 2, the highest occupied molecular orbital (HOMO) in the equilibrium structure is well described as a completely localized π orbital of cyclopentadienide, while the lowest unoccupied molecular orbital (LUMO) is a completely localized π^* orbital of cyclopropenium. In the TS structures, on the other hand, there is delocalization of the HOMO onto the three-membered ring that somewhat decreases the otherwise very large charge separation. This delocalization is assisted by the overlap of one formal LUMO of the isolated cyclopropenyl system with one of the formal HOMOs of the cyclopentadienyl system, i.e., ring-to-ring conjugation can occur when the planes of the two rings are twisted relative to one another by 90° (see Figure 2). This effect, potentially together with some electrostatic interaction, is presumably responsible for the additional shortening of the inter-ring bond in calicene compared to the uncharged reference systems above.

The very large, 7–9.6 D, dipole moments for the twisted structures indicate substantially increased charge separation compared to the planar equilibrium structures. The average increase in charge separation based on Mulliken population analysis at the DFT levels is 0.2 au. This is consistent with a greater dominance of the zwitterionic mesomer, since ideal planar conjugation of the two ring π systems is no longer possible. Examination of the Kohn–Sham wave functions for the twisted geometries indicates that for no functional is there a restricted \rightarrow unrestricted instability, i.e., there is no tendency for the TS structure to have biradical character. This observation indicates the critical nature of the aromaticity of the rings in the charge-transfer limit, since rotation about standard, unconjugated C=C double bonds is well-known to go through a biradical TS structure. The tendency of the TS structure to maintain closed-shell-like character is consistent with a 2-electron-in-2-orbital picture in which the two orbitals are substantially different in energy, resulting in a charge-transfer ground state, as described in more detail below.

With respect to the energetics associated with bond rotation, there is near quantitative agreement between all levels of theory (Table 1) that the activation energy is about 40 kcal mol⁻¹ and the free energy of activation is about 37 kcal mol⁻¹. Thus, rotation about the double bond in calicene is more facile than about the double bonds in ethylene and stilbene by roughly 25 and 10 kcal mol⁻¹, respectively. The excellent agreement between the single-determinantal KS DFT, MP2, and CCSD-(T) predictions and the CASPT2 levels of theory is consistent

with a lack of any biradical character in the TS structure. From a multireference standpoint, the degree of biradical character may be evaluated from the size of the coefficient of the dominant aufbau configuration state function relative to other contributors. As shown in Figure 3, the CASSCF procedure predicts the single-reference character of **1** to increase with bond rotation, reflecting the increased dominance of the closed-shell ionic state, which is responsible for the low activation energy and large dipole moment change also shown in Figure 3.

Solvation Effects on Electronic Ground State. Because of the importance of the charge-separated mesomer in the resonance description of **1**, one expects that solvation effects on the properties of calicene may be significant. In particular, more polar media would be expected to stabilize charge separation. Data on the effects of benzene ($\epsilon = 2.2$) and aqueous ($\epsilon = 78.3$) solvation on the geometries and charge separations of the equilibrium and TS structures of **1**, as well as on the rotational barrier, were computed using the conductorlike PCM continuum solvation model (Tables 2 and 3). Given the qualitative similarity of all of the DFT (and post-HF) results, we restrict our analysis here to results obtained at the PBE level.

Considering aqueous solvation first, the effects of the surrounding medium on the planar equilibrium structure include an increase in the length of all formal double bonds and a decrease in the length of all formal single bonds, i.e., bond alternation is reduced, consistent with an increase in zwitterionic character at the expense of the Kekulé structure. The magnitude of the effect is about 0.005 Å per bond, which leads to a decrease in the bond alternation parameters for each ring of about 0.01 Å. This geometric alteration is accompanied by increased charge transfer, whether measured by the ring Mulliken charges, which increase in magnitude by about 0.1 au, or by the electrical dipole moment, which increases by about 2 D.

Aqueous solvation effects are still larger on the TS structure in terms of reducing bond alternation in the five-membered ring. In the three-membered ring, bond alternation actually increases somewhat, which seems paradoxical. However, the comparison is less clear here because aqueous solvation causes the TS structure to have *C*_{2v} symmetry, i.e., the pyramidalization of the three-membered ring observed in the gas phase is eliminated. As noted for the equilibrium structure, the degree of charge transfer between the rings is significantly increased by aqueous solvation: the ring Mulliken charges increase in magnitude by 0.26 au and the electrical dipole moment increases by almost 5 D. The greater polarity of the TS structure causes its solvation free energy to be more negative than that of the equilibrium structure by 6.8 kcal mol⁻¹, which is nearly 20% of the rotational activation free energy.

As expected, solvation effects in benzene are qualitatively similar to those in water, but reduced in magnitude by a substantial degree owing to the smaller dielectric constant of the aromatic solvent.

Gas-Phase Calculations of Electronic Excited States. The first two singlet and triplet excited A1 and B2 states have been calculated at the MS-CASPT2 level on the optimized CASPT2 geometries (Table 4). TDDFT calculations were also examined. However, most of the lower energy excited states have associated with them a substantial amount of ring-to-ring charge-transfer character. Currently available functionals are well-known to underestimate the energy of charge-transfer excitations.⁵¹ and calicene proves no exception. Predicted TD-DFT excitations are as much as 2 eV lower in energy than corresponding

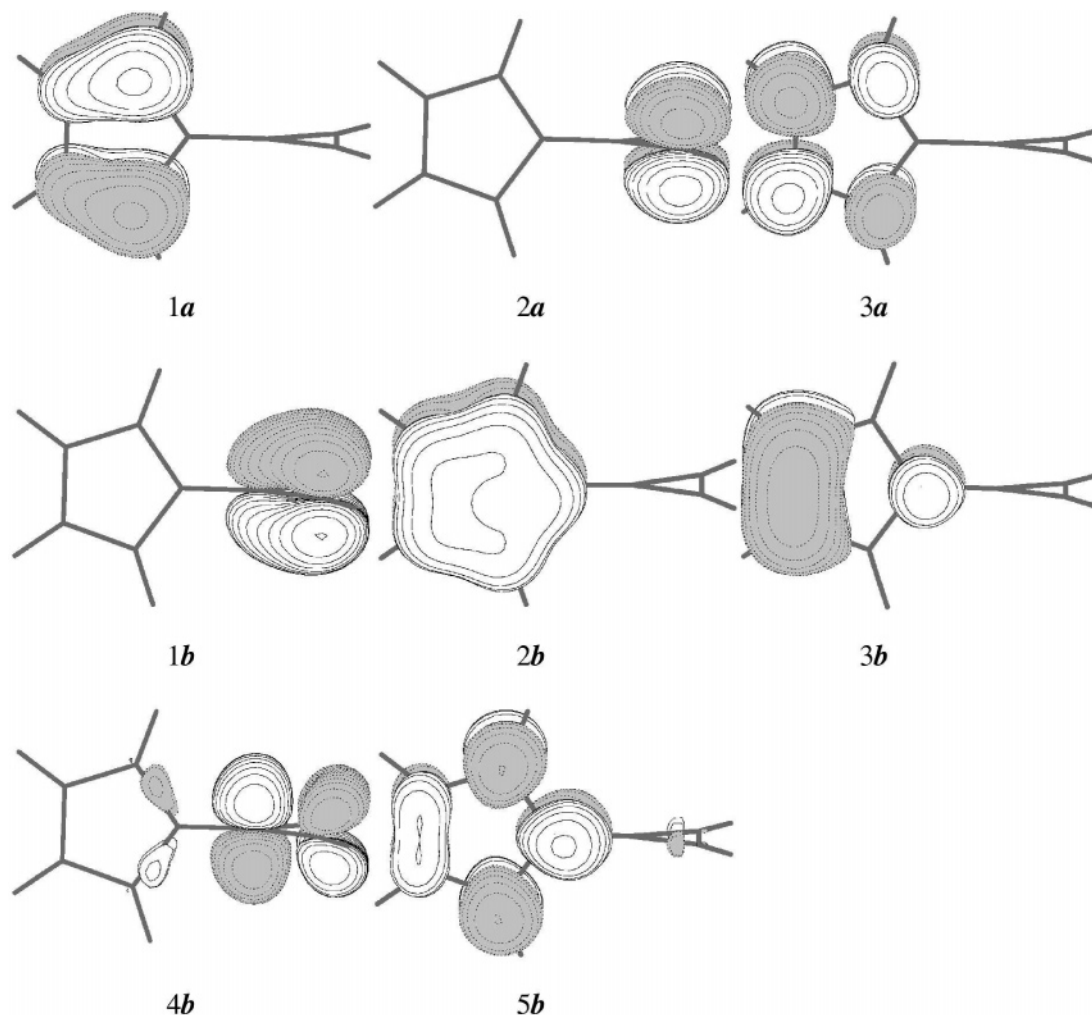


FIGURE 5. Molecular orbitals in the active space for the twisted TS structure of calicene.

predictions at the MS-CASPT2 level, and on that basis we will not discuss the TD-DFT level of theory further.

The values obtained for the 1A transitions (3.83 and 4.93 eV) can be compared with prior predictions of 3.81 eV⁷ for the first transition and 4.18 and 4.39 eV for each of the two.⁸ For the 1B transitions (3.84 and 4.03 eV) the same comparison is to 4.34 eV⁷ and 3.57 and 3.93 eV.⁸ The MS-CASPT2 values for the 1A states differ substantially from predictions made at the 3×3 CI (two electrons in two orbitals) semiempirical level (4.44 and 7.43 eV).⁹

Most of the excited states are well characterized as single excitations within the CASSCF active space (Figure 4). Thus, state $2-^1A$ is characterized by an excitation from orbital $1a$ to orbital $2a$, which corresponds to a charge-transfer from the five- to the three-membered ring. The resulting state has a dipole moment of sign opposite (-2.68) to that of the ground state. The occupation numbers of the $1a$ and $2a$ orbitals are close to 1 in the excited state (see Supporting Information, S15–S19), so it has essentially pure diradical character, as proposed by Takahashi.⁹

The $3-^1A$ state involves excitation from orbital $3b$ to orbital $4b$, with some contribution from a $1a$ to $2a$ excitation. With

these two components, and noting that the molecular orbitals belonging to the b irreducible representation (irrep) are more delocalized, the orbital occupation numbers for the $3-^1A$ state take on various non-integer values, i.e., this state is not a pure diradical. However, from the greater dipole moment, we can deduce that this state has a stronger zwitterionic character than the ground state, as was also observed by Takahashi.⁹

The remaining excited states are all dominated by a single electronic excitation and are well described as diradicals. On the basis of their dipole moments, they all exhibit charge-transfer character, in particular those dominated by transitions involving the localized molecular orbitals belonging to the a irrep.

The natures of the excited states in the twisted TS structure (Table 7) are more easy to understand as all active orbitals (Figure 5) are now well localized on the three- or five-membered rings, and all excitations exhibit a strong charge-transfer character involving transitions from orbitals localized on the five-membered ring ($1a$, $3b$) to orbitals localized on the three-membered ring ($2a$, $4b$). The excited-state dipole moments are all strongly reduced from the ground-state value (11.29 D), and in some cases they even change direction. The occupation numbers of all orbitals involved in the electronic excitations are close to 1.

The MS-CASPT2 potential energy curves of the excited states are shown in Figure 6 (the potential curve for the ground state

(51) Jamorski, C.; Foresman, J. B.; Thilgen, C.; Luthi, H. P. *J. Chem. Phys.* **2002**, *116*, 8761. Zyubin, A. S.; Mebel, A. M. *J. Comp. Chem.* **2003**, *24*, 692.

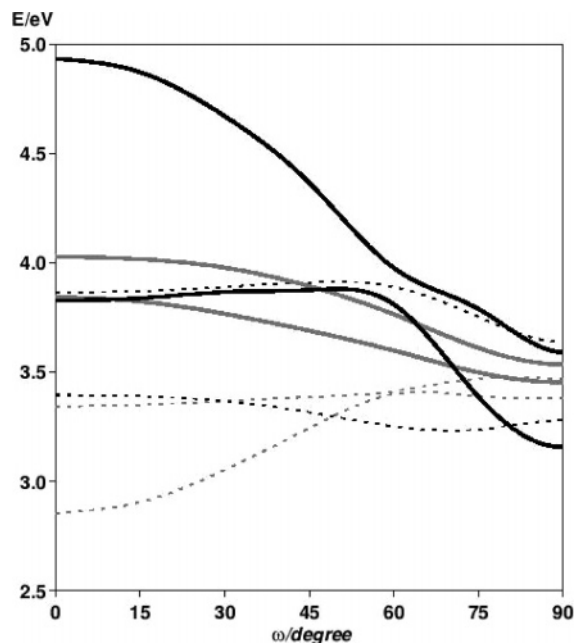


FIGURE 6. MS-CASPT2 adiabatic excited-state potential energy curves of **1**: (black solid line) 1A ; (black dashed lines) 3A ; (gray solid lines) 1B ; (gray dashed lines) 3B .

is shown in Figure 3 along with its properties). The shapes of the potential curves for the ground and first excited 1A states are in good agreement with those obtained at the semi-empirical level,⁹ whereas that for the third 1A state differs substantially both in energy and shape.

Figure 6 shows conical intersections between the 2- and 3- 1A states and the two 3B states, both near rotation angles of 60°. These are associated with inversions in the order of the dominant configurations: from planar to 45°-twisted calicene, excitations from orbital 1a characterize the lower states (see Supporting Information), whereas nearer the twisted TS structure the lower states are dominated by transitions from orbital 3b (compare also Tables 4 and 5). These crossings introduce strong interactions between the states so that a multistate treatment in the CASPT2 is required in order to properly describe their respective energies.⁴²

Figure 6 and a comparison of excitation energies in Tables 4 and 5 indicate that most of the electronic transitions are red-shifted in the twisted TS structure compared to the planar equilibrium structure. This reflects a reduction in the HOMO–LUMO gap (see Figure 7) for the former. From the shapes and energies of the active orbitals (Figures 5 and 7), the aromatic character of the active π molecular orbitals on the five-membered ring in the twisted TS structure can also be discerned. Thus, there is a fully bonding orbital, two degenerate HOMOs, and two almost degenerate LUMOs, in accord with the classical Hückel description of cyclopentadienide.

It is interesting to compare calicene to ethene, styrene, and stilbene with respect to the nature of singlet electronic states as a function of the torsional angle about the central double bond. The ground state of the 90°-twisted calicene shows a strong zwitterionic nature, whereas its singlet excited states are all diradicaloid. By contrast, for ethene and its derivatives, the opposite occurs: the ground states are diradicals, and the first singlet excited states are zwitterionic.^{52,53} This happens because in the 90°-twisted ethene, the π orbitals become degenerate.⁵⁴

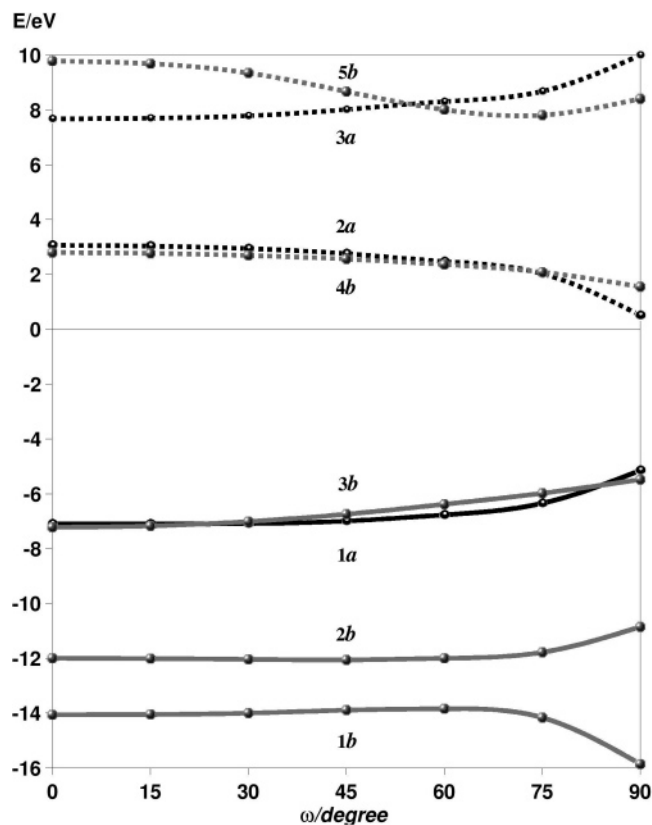


FIGURE 7. One-electron energies (eV) of the active molecular orbitals: (black lines) a -symmetry orbitals; (gray lines) b -symmetry orbitals.

In the case of calicene the active molecular orbitals never become degenerate (Figure 7) but are always well energetically separated so that the ground state of calicene is always a closed shell. Calicene has some similarity, then, with the case of aminoborane.^{55,56} In the 90°-twisted TS structure geometries, both molecules show a “hole-pair” ground state S_0 and a “dot-dot” diradical excited state S_1 . Thus, in the transition state, the ground state may be described as a twisted internal charge-transfer (TICT) state. Such states are usually excited states but the large separation of frontier orbitals in calicene and aminoborane ensures a hole-pair closed-shell ground state all along the rotational coordinate.

The location of the minimum at the twisted TS structure on the 2- 1A potential energy curve (Figure 6) suggests a possibly efficient photoisomerization, i.e., rotation around the central double bond induced by an electronic transition. Transition from the ground state to the 2- 1A state is predicted to have a low oscillator strength (Table 4); however, a transition to the 3- 1A state followed by an internal conversion to the 2- 1A state could be an alternative. To investigate this possibility further, we optimized geometries for the 2- 1A state with various twist angles

(52) Salem, L. In *Electrons in Chemical Reactions: First Principles*; Wiley & Sons: New York, 1982; pp 72–75.

(53) Molina, V.; Merchán, M.; Roos, B.; Malmqvist, P.-Å. *Phys. Chem. Chem. Phys.* **2000**, 2, 2211–2217.

(54) Michl, J.; Bonačić-Koutecký, V. In *Electronic Aspects of Organic Photochemistry*; Wiley & Sons: New York, 1990; pp 117–118, 310–314.

(55) Michl, J.; Bonačić-Koutecký, V. In *Electronic Aspects of Organic Photochemistry*; Wiley & Sons: New York, 1990; pp 219–222.

(56) Michl, J.; Bonačić-Koutecký, V. *J. Am. Chem. Soc.* **1985**, 107, 1765–1766.

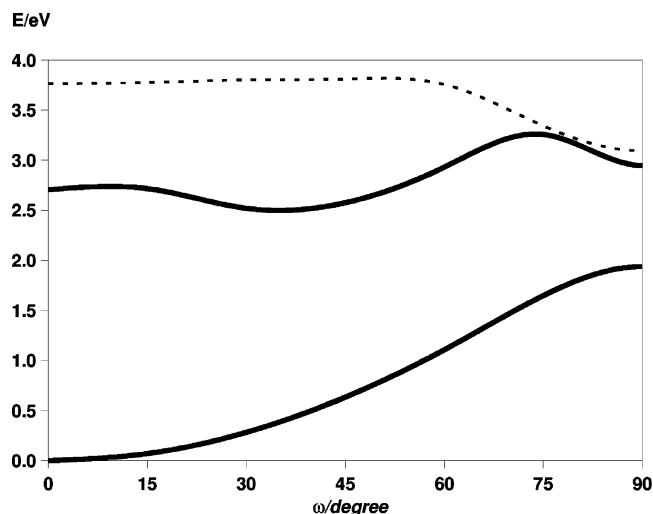


FIGURE 8. Photoisomerization of calicene. MS-CASPT2 adiabatic electronic potential curves of **1**: (solid lines) ground ($1^{-1}A$) and first excited ($2^{-1}A$) states with all geometric degrees of freedom other than torsion relaxed; (dashed line) excited state ($2^{-1}A$) at the optimized geometries for the ground state (as in Figure 6).

at the MS-CASPT2 level (including all three A states in the state average CASSCF, a level shift of 0.25 au, and a $3s2p1d/2s1p$ contracted basis set; single point energies were computed with a $4s3p2d/3s1p$ contraction). The potential curves for the $1^{-1}A$ and $2^{-1}A$ states are shown in Figure 8. The relaxed $2^{-1}A$ curve is quite different from that obtained by vertical excitation from ground-state geometries. The two geometries of these states are very different (Supporting Information, S27) as a consequence of the different natures of the wave functions: diradicaloid for the excited-state and closed-shell with increasing zwitterionic character for the ground state.

Optimization of the geometry of the $2^{-1}A$ state at a twist angle of 75° lowers its CASPT2 energy and rises the CASPT2 energy of the ground state. As a result, a strong interaction between these two states occurs and raises the energy of the $2^{-1}A$ state so that a rotational barrier is introduced relative to an equilibrium structure having a twist angle of about 40° . Assuming rapid vibrational relaxation, an activation energy of 0.9 eV (21 kcal mol $^{-1}$) would need to be overcome to reach the 90° twisted structure, from which fluorescence or nonradiative transitions might lead to rotational isomerization. These same processes will drain the population of the 40° minimum and would be expected to significantly reduce the efficiency of photoisomerization.

Solvation Effects. Excitation energies at the MS-CASPT2 level were also computed for the planar and twisted TS structures of **1** in benzene and water as represented by the nonequilibrium polarized continuum model (Tables 6 and 7). For the planar equilibrium structure, most excitations are blue-shifted in solution, with the magnitude of the shift increasing in water compared to benzene. This trend is generally expected for a polar molecule, since the ground state is in equilibrium with the solvent, whereas the vertically excited state is in equilibrium only with the electronic response of the surrounding solvent. In the case of **1**, moreover, all of the excited states except for $3^{-1}A$ have dipole moments that are either smaller than that for the ground state or are indeed reversed in direction (by charge transfer) and possibly quite large. In the latter instance, the frozen component of the solvent reaction field

destabilizes the excited state and enhances the blue shift. Thus, for the $2^{-1}A$ state, which has one of the largest reversed dipole moments, blue shifts of 0.26 and 0.62 eV are predicted in benzene and water, respectively. The aqueous effect is particularly large because the high dielectric constant of the solvent increases the relaxed dipole moment of the ground state to 5.06 D (cf. 3.30 D in the gas phase), and the slow component of the reaction field in water is a more significant fraction of the total reaction field than it is in benzene.

The $3^{-1}A$ state exhibits different behavior. The dipole moment of this state is larger than that of the ground state. As the excited-state dipole moment continues, by symmetry, to be perfectly aligned with that of the ground state, its interaction with the slow component of the reaction field is favorable and larger in magnitude than that of the ground state. As a result, this absorption in solution is *red*-shifted relative to the gas phase, by 0.10 and 0.20 eV in benzene and water, respectively. The combination of blue and red shifts causes the $2^{-1}A$ and $3^{-1}A$ states to approach one another closely in water.

In the twisted TS structure, the ground electronic state has a very large dipole moment, whereas all of the excited states have dipole moments of less than 1.5 D. Given these small excited-state dipole moments, all of the excited states have rather similar interactions with surrounding solvent, and the result is a near constant blue shift of about 0.1 and 0.2 eV for all excitations in benzene and water, respectively.

Conclusions

Density functional theory and post-HF methods such as MP2 and CASPT2 agree well for ground-state properties of calicene, including the activation energy for rotation about the inter-ring double bond, which is substantially reduced by the aromatic stability of the closed-shell charge-transfer-like transition-state structure. Polar solvation decreases the barrier still further, as would substituent effects that provide additional stability for charge transfer.

Time-dependent DFT is not appropriate for the computation of excitation energies in calicene because of the substantial charge-transfer character in many of the low-energy excitations. However, the more rigorous MS-CASPT2 model provides significant insights into the electronic excited states. All of the studied low-energy excited states (with the exception of $3^{-1}A$) have diradical character that persists over the full rotational coordinate. The gas-phase electronic transition with the largest predicted oscillator strength (0.3) leads to the second excited singlet A state ($3^{-1}A$) and occurs at 4.93 eV (251 nm). Excitation to the $2^{-1}A$ state (or internal conversion to it from the $3^{-1}A$ state) could in principle lead to a *cis*–*trans* photoisomerization about the double bond joining the two rings. However, the presence of an energy barrier of 0.9 eV (21 kcal mol $^{-1}$) on the relaxed potential energy curve for the $2^{-1}A$ state suggests that this process is not likely to be particularly efficient.

Acknowledgment. Local funding from the Torino University, for the year 2005, is gratefully acknowledged by G.G. Financial support was also provided by the U.S. (CHE-0610183) and Swiss (200021-111645/1 and P10I2-112994) National Science Foundations.

Supporting Information Available: Cartesian coordinates of all structures and their absolute energies (hartrees, kcal mol $^{-1}$, and eV) are given. This material is available free of charge via the Internet at <http://pubs.acs.org>.

JO062420Y